Colloids and Surfaces A: Physicochem. Eng. Aspects 349 (2009) 102–109

Contents lists available at ScienceDirect

Colloids and Surfaces A: Physicochemical and Engineering Aspects

journal homepage: www.elsevier.com/locate/colsurfa

Porous polymer films cast from latex–glucose dispersions

Andrew Fogden*

Department of Applied Mathematics, Research School of Physical Sciences and Engineering (RSPE), Australian National University, Garran Rd, Canberra ACT 0200, Australia

ARTICLE INFO

Article history:
Received 12 June 2009
Received in revised form 4 August 2009
Accepted 5 August 2009
Available online 11 August 2009

Keywords:
Porous polymer
Latex
Film formation
Pore forming agent

ABSTRACT

Macroporous films of glassy polymer are prepared from stable aqueous dispersions of latex with dissolved glucose, coated on a carrier substrate and dried at elevated temperature to a hybrid film, followed by water immersion to leach out the glucose and any redispersible latex. Temperature and time of drying must be tailored to facilitate local coalescence of latex particles by glucose expulsion while avoiding complete demixing of the two phases. The conditions for which mutual interpenetration of locally film-formed latex and glucose networks can be kinetically locked-in to maximize film yield and porosity are elucidated as a function of glucose/latex content. The porous films were analyzed gravimetrically and by UV–vis spectroscopy and scanning electron microscopy. They possess a disordered connected network of sub-micron pores graded in the film thickness direction, with accessibility decreasing from upper to lower surface due to upward transport of mobile glucose by capillarity and convection.

1. Introduction

A latex is an aqueous colloidal dispersion of spherical polymer particles synthesized via emulsion polymerization. By this process a broad range of polymers and copolymers at high molecular weight can be packaged into monodisperse particles, surface stabilized to yield aqueous dispersions with relatively low viscosity even at high concentrations. This combination of properties confers on latex systems a spectrum of industrial applications and a vast scientific literature, either directed at these applications or more fundamental research using latex as a model colloid [1–7]. One of the highest-volume industrial uses of film-forming latexes is in paper coatings, where an aqueous suspension of micron-sized mineral pigment particles and sub-micron latex is layered on the paper surface and dried to a porous coat, with latex serving to bind the pigment particles to each other at their contact points and bind the coat to the substrate [8]. An example of more recent research thrusts, targeting higher-end applications such as advanced optical devices, involves preparation of colloidal crystals of non-film-forming latex and deposition of an inorganic phase in the interstices to yield "inverse opal" porous frameworks on removal of the sacrificial latex template [9]. In common with these two examples, the present study also focuses on macroporous films with sub-micron pore sizes, however with the distinction that latex itself now constitutes the sole solid phase.

The sub-processes by which a wet film of milky latex dispersion transforms on drying to a transparent, continuous and non-porous film are generally idealized as a sequence of three stages [1–7,10]. In the first stage the evaporation of water from the free surface(s) increases the dispersion concentration until latex particles consolidate and order into a close-contacting, close-packed structure. As water continues to be lost from between the latex particles, the second stage of latex particle deformation takes place, in which the original spheres are compacted to space-filling polyhedra, thus eliminating their interstices. For this deformation to occur, the drying temperature must exceed the minimum film formation temperature of the latex, which is typically close to its glass transition temperature. The exact mechanisms responsible for compaction will depend on the latex system and drying conditions, being driven by a combination of interparticle van der Waals attractions acting to reduce the latex interfacial area exposed to the intervening water (wet sintering) or air (dry sintering) and the longer-range capillary attraction of the concave air–water meniscus bridging them during evaporation. In the final stage of coalescence the compacted particles of relatively hydrophobic polymer must overcome the barrier of their more hydrophilic stabilizing layers of polymer, surfactant and ions to facilitate interdiffusion of polymer chain-ends to form a seamless film with mechanical strength and resisting redispersion. These three stages for formation of a coherent polymer coating often occur continuously and with increasing overlap for drying temperatures increasingly exceeding the minimum film formation temperature.

In some applications for which latex is the principal or only component of the film, e.g. water-borne paint layers or dispersion coatings, the film is designed to be non-porous to maximize strength and transparency and provide a barrier across which undesirable ingress of molecules is restricted to only very slow diffusional transport. Other applications in release, separation,

* Tel.: +61 261254823; fax: +61 261250732.
E-mail address: andrew.fogden@anu.edu.au.

0927-7757/$ – see front matter © 2009 Elsevier B.V. All rights reserved.
doi:10.1016/j.colsurfa.2009.08.003

catalysis and sensors require creation of film porosity for more rapid, controlled permeation, e.g. of a drug or nutrient from a bead thus coated. Latex films cast from aqueous dispersion can be rendered porous via a number of strategies. The simplest approach, employing only a single, unmodified latex dispersion, is partial coalescence, i.e. sufficient to locally merge particles across their contact zones to instill some film integrity, but insufficient to eradicate all interstitial porosity [11]. A related approach analogous to paper coating structures entails mixing larger non-film-forming latex with lesser amounts of smaller film-forming latex to serve as glue [10,12], or use of core–shell latex with a hard core and soft shell. Another general strategy uses addition of a pore forming agent to the latex dispersion, which is thus incorporated into the latex film during film formation and removed afterwards [11–15]. Liquid agents must be water miscible and not destabilize the latex dispersion, and be readily removed from the film by leaching in water. The resulting pore space and permeability is dictated by the relative amount of additive, its compatibility and mobility during latex film formation and the degree of pore collapse during leaching and post-drying. Examples of pore forming agents tested are glycerol [11,14], sucrose [12–14], dissolvable second latex [14] and urea [15]. In these studies the porous latex films obtained are generally structurally similar to the partially coalesced state mentioned above, exhibiting discernable, individual latex particles with somewhat increased interstitial porosity and a slightly looser packing. Thus the main purpose of the pore forming agent was to increase the flexibility in choice of latex formulation and drying conditions to achieve partial coalescence.

Other strategies for creating porous latex can result in a more substantial alteration of the sub-micron pore space or the overall macroscopic form of the body. On addition of an immiscible oil phase to a diluted latex aqueous dispersion, emulsion droplets can be stabilized by a monolayer of latex particles at the oil–water interface. Partial wet sintering of the latex and removal of the two liquids leads to hollow capsules with shell porosity by virtue of the remaining latex interstices [16]. Exposure of latex to solvent vapor can induce more drastic changes to pore morphology. A polystyrene latex dispersion contacted by acetone vapor could under certain conditions produce a foam-like porous coagulum [17], while exposure of a pre-formed colloidal crystal of core–shell polystyrene-polyHEMA latex to vapor of a good solvent for polystyrene led to an inversion transition to a polymer net [18].

The current study reassesses the scope for transformation of the pore space of latex films using pore forming agents. In particular, the agent used, glucose, and its addition levels are similar to those investigated previously, however higher temperatures of wet film drying and curing are now investigated. These conditions serve to more fully coalesce neighboring latex particles and expel the interstitial glucose to form a continuous, coherent sub-micron network of latex intertwined with a similar pore network. Conditions for achieving the optimal balance between latex film formation and glucose demixing are determined, and the underlying mechanisms at play are discussed. The simplicity of the procedure and robustness of the films obtained are favorable for inexpensive industrial processes and porous polymer products with applications ranging from adhesion promoters to sensors.

2. Experimental

2.1. Materials

The emulsion polymer used was a commercial latex product, HPS 61 (Dow Chemical, Horgen, Switzerland), comprising a spherical core based on styrene–butadiene and stabilized by a copolymerized carboxylic acid corona, with average particle size 130 nm and high monodispersity in size and sphericity. This hydrophilic, anionic latex is delivered as an aqueous dispersion, together with anionic and non-ionic surfactants, at pH 7.0, with solids concentration 49.4 wt% and viscosity 115 mPa·s. The latex has a glass transition temperature of 26 °C, and thus its film formation entails drying at temperatures above ambient (22 °C). An aqueous stock solution of D-glucose (anhydrous, 99%, Univar) of concentration 0.85 g/ml was prepared using deionized water from a Millipore Milli-Q reverse osmosis system (as used throughout this study). From this solution, latex–glucose aqueous mixtures were prepared at the four glucose/latex mass proportions (percentage glucose dry mass per latex dry mass) of 15, 20, 25 and 30%, in all cases with total mass fraction of dispersed latex solids fixed at 37.5 wt%. These mixtures were prepared by first adding to the latex dispersion the appropriate amount of water, then adding the glucose stock solution dropwise under slow stirring. All four dispersions remained stable in screw-top jars off-stirring over the entire period of observation (approximately 2 months), and possessed viscosities similar to that of the parent latex sample. Coating of these dispersions was performed on microscope glass slides of dimensions 76.2 mm × 25.4 mm.

2.2. Preparation and analysis of porous latex films

A drop of the particular latex–glucose aqueous mixture, of fixed target mass 0.027 g was applied onto a pre-cleaned, pre-weighed glass slide and manually spread uniformly over its full width along approximately 60 mm of its length. The wet coated slide was then transferred directly to an air oven preheated to the desired temperature for drying and curing for the desired duration. Upon removal, the sample was re-equilibrated to ambient conditions for 10 min, reweighed, then immersed in a covered water bath of 50 ml volume in a Petri dish of 90 mm diameter to leach the glucose from the film under quiescent conditions for approximately 150 min. The water plus dissolved glucose and any redispersed or dislodged latex was then removed by pipette and the slide with its residual latex coat was dried ambiently prior to re-weighing and further analyses. Slow quiescent leaching was employed to avoid film break-up or folding due to mixing stresses, which would otherwise complicate the interpretation of the subsequent analyses.

Generally, higher glucose/latex proportions or lower drying temperatures or shorter durations lead to more substantial redispersion of the latex in the water bath and thus to lower yield of latex film on the slide, while the opposite extremes favor complete macroscopic phase separation of glucose during latex film formation, resulting in a non-porous transparent latex film. For each glucose/latex proportion a series of three drying temperatures (in steps of 10 °C) was tested, each for the four durations of 5, 10, 20 or 30 min. In particular, the midpoint of the temperature range was chosen such that the lowest temperature (10 °C below this) gave substantial redispersion of latex (at least for the shorter durations) while the highest temperature (10 °C above this) tended to give complete phase separation (at least for the longer durations). Accordingly the midpoint temperature was chosen as 90, 110, 130 and 140 °C (±3 °C) for glucose/latex proportions of 15, 20, 25 and 30%, respectively, in order to traverse this full range of behavior for each.

From the gravimetric analysis the percentage of latex retained in the film relative to its starting mass was directly calculated. A UV–vis scanning spectrophotometer (Shimatzu UV-3101PC) was used to quantify the resulting loss in film transparency due to micropores created and vacated by glucose. The slide was lightly clamped in its sample holder perpendicular to the incident beam, film side facing forwards, and with a clean glass slide in the reference cell. Transmission spectra were recorded with a 1 nm slit width over the interval 800–300 nm, with six such spectra obtained per sample piece by laterally translating it along the long axis of the

slide to obtain a representative average over the full residual coated area. Latex film morphology was imaged at high magnification using a field emission scanning electron microscope (FESEM, Zeiss UltraPlus Analytical) under high vacuum operating in secondary electron mode at 3 kV. Representative film pieces were selected by scoring and snapping the underlying glass slide, which was then mounted on an aluminum stub using a double-sided adhesive carbon tab. To investigate the morphology at the underside of the film, sample pieces were re-immersed in water, removed and partially dried ambiently, at which time an aluminum stub with adhering carbon tab was contacted with the drier top surface to result in clean delamination of the wetter bottom surface of the film from its glass carrier. In both cases all samples were lightly pre-coated with platinum to minimize beam charging.

For one sample, with glucose/latex proportion of 25% and dried at 120 °C for 30 min, its pore space was probed using mercury porosimetry (Micromeritics AutoPore IV). This technique requires freestanding porous film in sufficient quantities to vacate a substantial fraction of the penetrometer stem volume during intrusion. To this end the residual latex coat was cleanly rolled off its backing slide while in the wet state directly after removal from the water bath, then dried ambiently, with this procedure repeated for 33 slides to yield 0.281 g of dry porous film. The film pieces were packed into the bulb of the penetrometer, which was subsequently filled with mercury and the pressure ramped up, first from 0.53 to 30 psi then on up to 30,000 psi, during which the volume of mercury progressively exiting the stem to enter the bulb and intrude the sample was monitored.

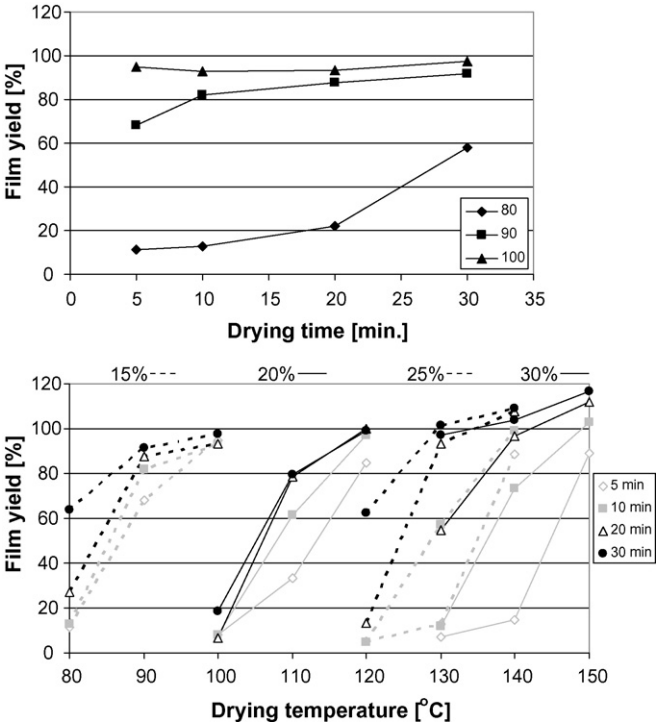

Fig. 1. Gravimetric film yield, plotted as a function of drying time for the glucose/latex proportion of 15% at the three drying temperatures of 80, 90 and 100 °C (upper diagram), and all results for the four glucose/latex proportions (15, 20, 25 and 30%) at their three respective temperatures and the four drying times (lower diagram).

3. Results

3.1. Yields of latex film

From the measured coat weight after oven drying and the known total solids content of the latex–glucose mixture, the wet mass of the coat originally applied to the slide was determined. Over all 48 samples prepared and analyzed, the average wet mass was 0.0272 g with a standard deviation of 0.0013 g, i.e. coefficient of variation of only 4.7%. Thus the average applied mass of latex per sample was 0.0102 g, and varied little between samples. This corresponds to an average latex coat weight of 6.68 g/m^2, equivalent to an average latex thickness of 6.55 μm if regarded as a non-porous layer, i.e. ignoring the presence of glucose. Fig. 1 summarizes the results for the gravimetrically determined film yield for each sample, defined as the percentage mass of residual film on the slide substrate, after removal from the water bath and ambient drying, relative to the dry-equivalent mass of solid latex originally applied. In particular, the upper diagram in Fig. 1 plots film yield for the 15% glucose/latex mixture for the four drying times at each of its three drying temperatures. For all four glucose/latex compositions the three curves versus drying time at low, intermediate and high temperature are qualitatively similar. To within experimental error, film yield always increases with temperature and drying time, with the slope versus drying time increasing for the low temperature and decreasing for the two other temperatures as the upper plateau of maximum yield is approached, especially at the high temperature. For glucose/latex proportions of 25 and 30%, this plateau value exceeds 100%, implying that a fraction of glucose remnants are present in the film after the water bath. This is due to the oxidative decomposition of glucose at the higher temperatures and longer durations employed at these two highest proportions and accompanying decrease in room-temperature water solubility of the products.

The lower diagram in Fig. 1 presents the film yield for all samples, now plotted versus drying temperature with four curves for the four durations, and alternating from dashed to solid lines with increasing glucose/latex proportion to distinguish the families. Again it is apparent that film yield increases with both temperature and duration of drying for each family, and decreases with increasing glucose/latex proportion (compared for a fixed time at the common temperature of 100, 120, 130 or 140 °C where two families overlap).

3.2. Film transparency

After oven drying all samples were uniformly transparent continuous films, either colorless or brown tinged for the higher temperatures and longer durations due to glucose decomposition. On immersion in the water bath, sample transparency progressively decreases as glucose dissolves and diffuses out of its microdomains in the film, increasing the refractive index contrast between these water-filled domains and the surrounding styrene–butadiene matrix. Film samples containing micro-segregated glucose are thus rendered milky translucent in the bath, while samples giving lower yields whiten as the separation between latex particles or insufficiently coalesced fragments increases on redispersion or suspension. Samples for which glucose completely demixes from the latex film during drying remain transparent in the bath and on subsequent ambient drying. The milky translucent films increase strongly in whiteness and opacity, relatively uniformly across their length and width, on ambient drying as water evaporates from the microdomains. This is followed by a slight drop in opacity due to capillary and drying stresses collapsing or shrinking some less stable pores, despite room-temperature lying a little below the latex glass transition. In this final state the porous latex film is robust and not further affected if re-immersed in water and redried ambiently. Some studies [14] employ freeze-drying to avoid the pore closure on final

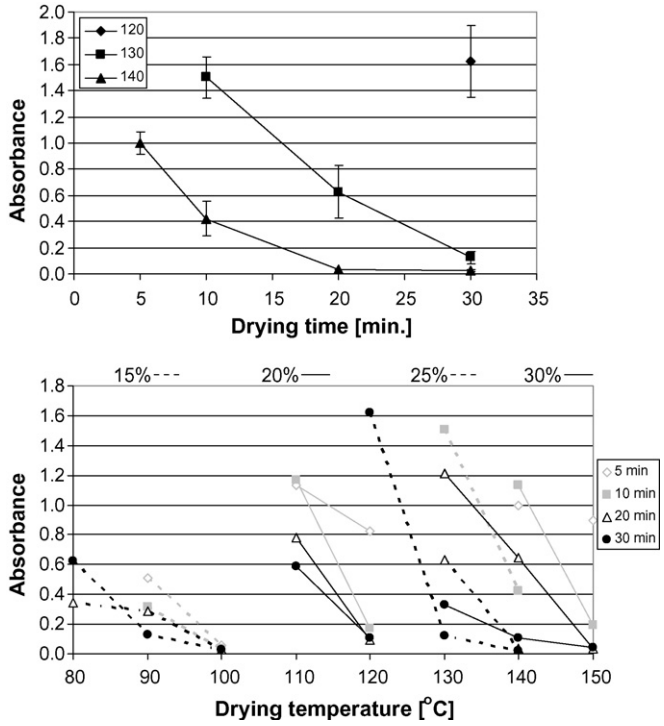

Fig. 2. Film absorbance at 800 nm, plotted as a function of drying time for the glucose/latex proportion of 25% at the three drying temperatures of 120, 130 and 140 °C (upper diagram), and all results for the four glucose/latex proportions (15, 20, 25 and 30%) at their three respective temperatures and the four drying times (lower diagram).

water evaporation, however the difference for our samples would only be small and ambient drying is more relevant to realities of industrial production and use of the materials.

In this final dry state transmission spectra were obtained by UV–vis spectroscopy for the subset of samples having a relatively high yield of coherent latex film, i.e. in excess of approximately 20% in Fig. 1. Care was taken to analyze only those subareas over which the film lay flat on its slide substrate, not doubled-over or creased. For all samples the absorbance decreases monotonically over the interval 300–800 nm, thus while only its value at the upper endpoint is presented here (giving best measurement precision), the trends would be identical irrespective of this choice. No corrections were made for the slight variation in film weight between samples (see above), the influence of which is dwarfed by the substantial differences due to glucose/latex proportion and drying conditions.

Fig. 2 presents the results of average film absorbance at 800 nm for each measurable sample, presented in the same format as Fig. 1, although now with the representative upper diagram in Fig. 2 corresponding to the glucose/latex proportion of 25%. The error bars in this upper diagram are the standard deviations over the six subareas analyzed on each sample film. These bars are quite large, and generally increasingly so for more highly absorbing samples, however the trends remain apparent. The absorbance plots are naturally unsuited to distinguishing slight differences in transmittances close to 100%, however such substantially transparent samples are of lesser interest in this study. Results in Fig. 2 should be compared to two reference latex film samples, prepared according to the same procedure as outlined above but in the absence of glucose and without the water immersion step. The first, oven dried at 120 °C for 30 min, gave an absorbance at 800 nm of 0.018 ± 0.004, which lies just below the values for the most transparent samples of the full matrix, namely at highest drying temperature and longest duration for each glucose/latex proportion. The second reference, only dried ambiently and thus non-film-formed, gave a value of 0.206 ± 0.012, lying substantially below that of most of our glucose-templated porous film samples, presumably mainly owing to the poor light scattering efficiency of its pores, lying well below 100 nm in size. A partially coalesced sample of this latex, i.e. of the structure typically obtained using pore forming agents in other studies [11–14], would exhibit absorbance intermediate to these two references.

In the upper diagram of Fig. 2 the results are thus presented for those 8 of the 12 samples at glucose/latex proportion of 25% which yielded sufficiently coherent latex film for measurement, i.e. omitting all but the longest oven duration at 120 °C and omitting the shortest duration at 130 °C. Absorbance clearly decreases with both temperature and time of drying and curing, in exactly the opposite manner of film yield, since these conditions favor latex film formation and glucose expulsion. The lower diagram in Fig. 2 evidences that this expected trend generally applies, within experimental error, to all glucose/latex proportions tested, and moreover that absorbance increases with glucose content when compared at fixed temperature (120, 130 or 140 °C) and time. Clearly the choice of conditions for preparation of porous latex via this approach entails a compromise between maximizing porosity and yield.

3.3. Morphology and measures of porous film

Strongest light absorbance is obtained for a glucose/latex proportion of 25%, in particular with the sample cured at 120 °C for 30 min (abbreviated 25%_120_30) being strongest of all. Fig. 3

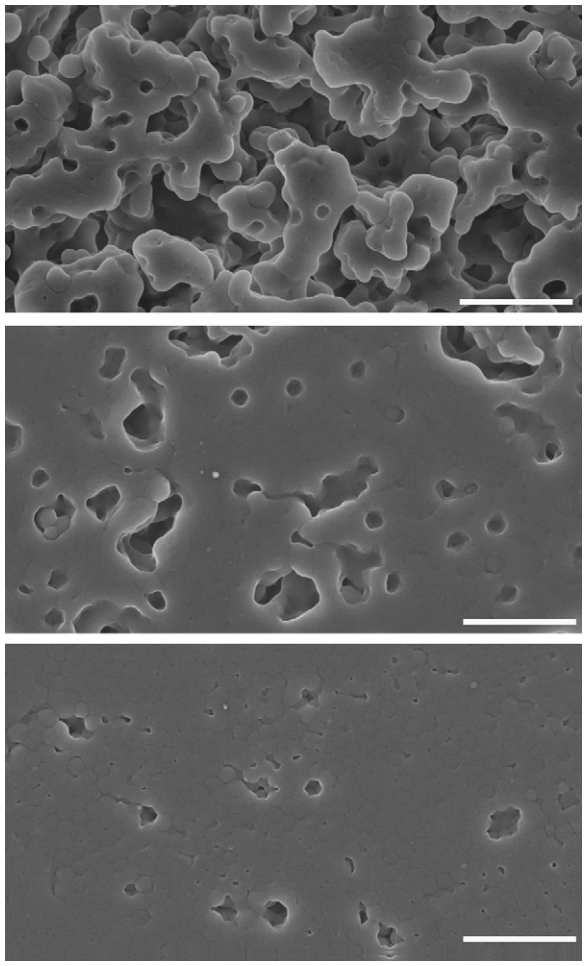

Fig. 3. FESEM topographical images of upper surfaces of porous latex films corresponding to the three samples (from top to bottom): 25%_120_30, 25%_130_30 and 25%_140_30. Scale bar is 1 μm in all micrographs.

displays representative FESEM topographical views, i.e. looking down on the free upper surface which faced air during drying and curing, for this porous latex film (top image) and its counterparts 25%_130_30 and 25%_140_30 for the two higher temperatures at this fixed glucose content and (maximum) drying time. For this sequence of three samples the average absorbance in Fig. 2 decreases strongly from 1.62 to 0.13 to 0.02, approximately an order of magnitude for each 10 °C increment. The interior of the film for 25%_120_30, visible through its surface pores, exhibits a connected network of coral-like agglomerates of coalesced latex, of thickness between one and several particle diameters (i.e. in the range 100–400 nm), and often sprouting dead-end nodules. The intervening pores vacated by the glucose are open and highly connected, but disordered and irregular in size and shape, without any facets suggestive of latex templated against glucose crystallites. Its upper surface, while containing large pores, also presents quite large, flat subareas of coalesced latex in Fig. 3. On increasing the curing temperature (middle and bottom images in Fig. 3) these flat subareas increase in prevalence to almost completely seal the surface for 25%_140_30. All indications from light absorbance are that bulk porosity has also been drastically reduced by temperature. Note that even at the highest temperature, latex particles are deformed but not completely coalesced at and near the upper surface. The surface vacancies in 25%_140_30 are polyhedral, indicating latex particles lost in the water bath rather than dissolution of a glucose microdomain. Thus expulsion of glucose to the upper surface at high temperatures appears to continue throughout the 30 min duration, leaving a sheath around some upper latex particles to hinder full coalescence or occasionally result in redispersion.

For this glucose/latex proportion of 25%, the two higher temperatures of 130 and 140 °C require much shorter curing times in order to reduce the excessive (pore-eradicating) film formation shown

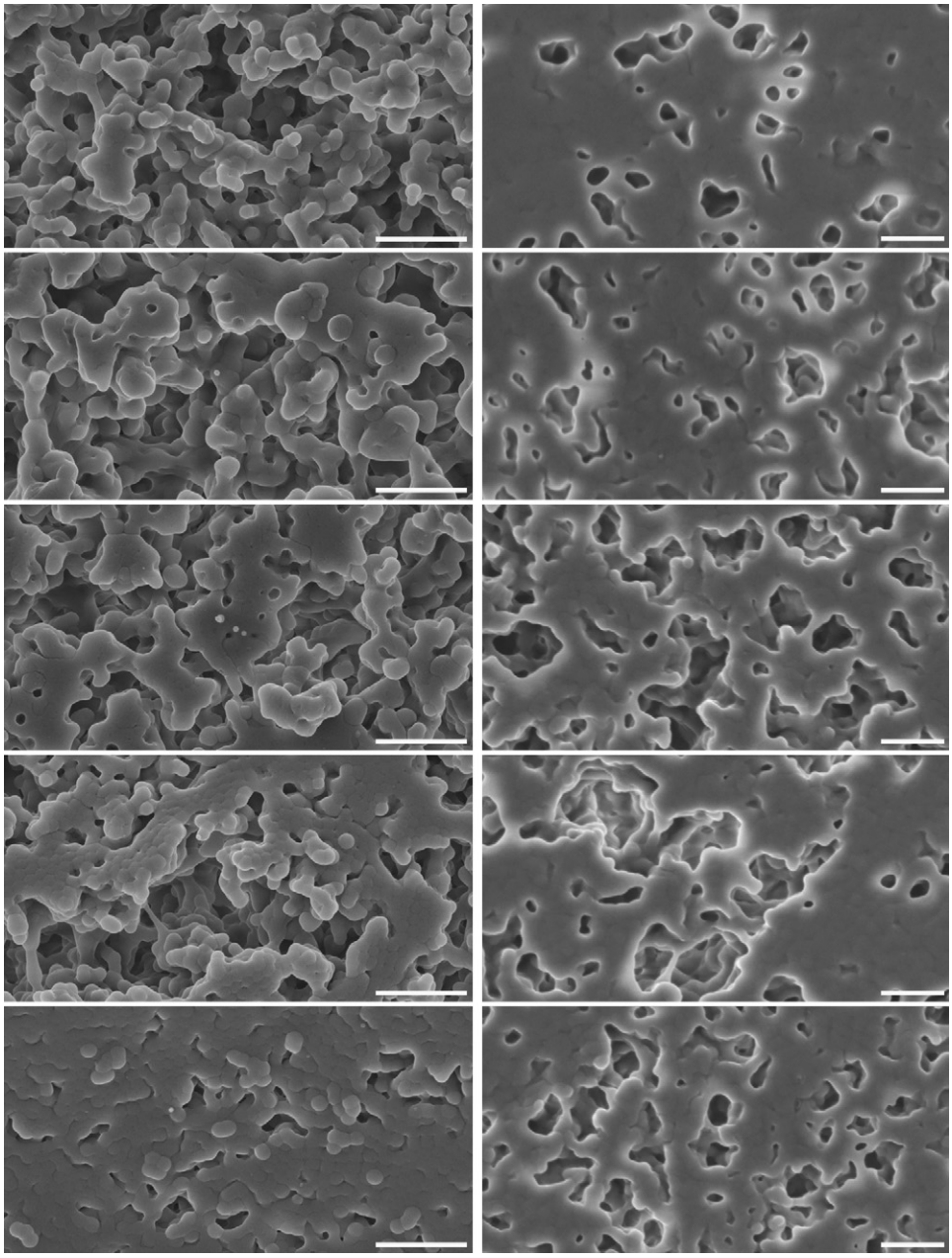

Fig. 4. FESEM topographical images of upper and lower (left and right column) surfaces of porous latex films of the five samples (from top to bottom): 25%_140_5, 25%_130_10, 25%_120_30, 20%_110_10 and 15%_80_30. Scale bar is 1 μm in all.

in Fig. 3. From Fig. 2 the durations giving strongest absorbance at these two temperatures are 10 and 5 min, respectively. The remainder of this section focuses on these three samples, 25%_120_30, 25%_130_10, and 25%_140_5, along with the samples 20%_110_10 and 15%_80_30 giving strongest absorbance at these two lower glucose contents. The identification of these five samples as most promising for their respective glucose contents holds irrespective of whether they are judged by film absorbance or its product with film yield to factor-in the above-mentioned compromise between maximizing porosity and yield. Representative FESEM micrographs of each sample are provided in Fig. 4, with upper and lower surfaces of each displayed in the left and right columns, respectively. It must be borne in mind that while the five samples are ordered with decreasing temperature from top to bottom in Fig. 4, glucose content and/or curing duration varies throughout.

For the 25%_120_30 sample (middle row of Fig. 4) the upper and lower surfaces are reasonably similar and thus the film appears quite symmetric about its midplane, albeit with somewhat lesser accessibility for the lower surface due to its larger, flatter subareas of coalesced latex. For the two higher temperatures (top two rows in Fig. 4) the effect of decreasing curing time more than cancels out that of increasing temperature to progressively increase accessibility of the upper surface. Both the size of the flat sealed subareas and the total fraction of the plane occupied by them decrease, so that the upper surface of 25%_140_5 (top left image in Fig. 4) displays an open coral-like latex morphology. On the other hand the reverse is true of the lower surfaces of these three samples with 25% glucose content, namely that increasing temperature now dominates decreasing curing time to progressively seal the surfaces, much in the manner of Fig. 3, and so increase asymmetry of their sides. The bottom two rows of Fig. 4 cannot be directly compared to the others, since their glucose contents, and thus their scope for building porosity, are reduced. The lowest temperature sample 15%_80_30 is the only one analyzed that displays a somewhat greater accessibility through its lower surface than its upper. Note generally in Fig. 4 that with decreasing curing temperature the degree of latex coalescence decreases, as expected.

While light absorbance provides one quantitative measure of the pore space of the glucose-templated latex films, this measure subsumes the individual roles of porosity and pore size. For this reason the technique of mercury porosimetry was tested on one sample, in particular 120_25%_30 yielding greatest light absorption. Although the total specific volume of mercury intruded into this porous latex film over the entire pressure range of 0.53–30,000 psi was high, namely 1.23 cm^3/g, the majority of this does not correspond to true internal porosity. In particular, the intrusion at low pressures is due to mercury progressively filling the gaps between the individual film pieces to envelop their external surfaces. At the highest pressures the measured intrusion is associated with collapse and compression of the original porous polymer structure. We thus limit the intrusion to that measured between 44.9 and 14800 psi, corresponding via the Young–Laplace equation to pore entrance diameters from 4.0 μm down to 12 nm, as all pores discernable from the FESEM micrographs lie within this range. The specific cumulative volume of mercury intruded, corrected in this manner, is plotted versus entry pore diameter in Fig. 5. The total volume intruded over this pressure subinterval implies a sample porosity of 10.8% and a median pore diameter of 0.58 μm. This porosity value is substantially lower than qualitative estimates from all FESEM images, presumably due to sample compression effects becoming significant even at low pressures and thus leading to underestimation. The median pore size is however qualitatively similar to that judged from the FESEM micrographs. This size is many times larger than mercury porosimetry values from latex films incorporating pore forming agents in other studies [14], which furthermore used larger latex spheres. This difference

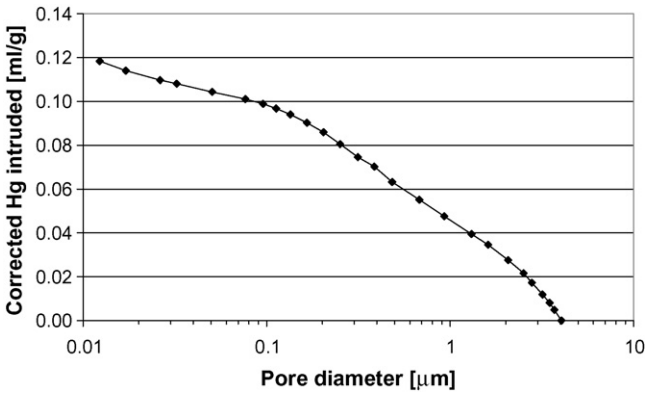

Fig. 5. Specific cumulative volume of mercury intruded into the porous latex film of sample 25%_120_30 as a function of its pore diameter inferred from the Young–Laplace equation.

emphasizes the distinction between pores created predominantly by latex interstitial glucose in the latter case and latex extruded glucose channels in our study.

4. Discussion

On oven drying, water evaporates initially from the flat upper surface of the wet coat, which then recedes to continue evaporation across the concavely curved air–water menisci between latex spheres at the surface. The under-pressure below these menisci acts to draw up the sub-surface latex, glucose and water, as does the upward convective current due to evaporation. Acting against these upward driving forces is the viscous resistance to flow and the Brownian motion of back-diffusion attempting to reduce any developing concentration gradient. In the case of relatively low temperature drying the evaporation rate is slower than the diffusion rate and the composition of all three components is maintained as uniform across the reducing thickness [1–7,10]. For this situation the presence of glucose will do little to influence the usual three-stage progression of latex film formation, other than to progressively increase viscosity and further slow evaporation of water [11,14,19]. A thickened honeycomb structure of hydrated glucose separating the rounded-polyhedrally deforming latex particles will result, with subsequent coalescence of some particle contacts and accumulation of glucose in interstices and at other contacts to block their coalescence. This model applies to the porous latex films obtained in most other studies of pore forming agents [11–14].

In contrast to these studies, most of our samples are dried and cured at substantially elevated temperatures. The strong convection will create a glucose concentration gradient, enriched near the upper free interface and depleted at the lower interface with the substrate, owing to its high mobility compared to the large and sterically hindered latex particles, as observed for other readily migrating additives [10]. The higher the temperature the steeper this gradient will be. Given that our wet coats are relatively thin, with an approximately 17 μm starting thickness, back-diffusion might be expected to be significant [4,7], however this very high glucose content near the upper surface fundamentally changes the nature of the ensuing film drying. The upper interstitial water loaded with glucose becomes a viscous plug, inhibiting evaporation and air invasion by downward movement of menisci, i.e. Haines jumps due to the increasing curvature of the water-starved meniscus exceeding the pore throat entry threshold. The situation is somewhat similar to the phenomenon of latex skinning [10], but with the distinction that glucose is highly hygroscopic. This acts to draw up water (and dissolved glucose) from the lower regions to maintain glucose hydration against evaporation. The dehydration

and glucose depletion of these lower regions will result in onset of their latex deformation and wet sintering [5] prior to substantial deformation in the upper realms heavily sheathed by glucose, i.e. the opposite of usual latex film formation.

Although the presence of glucose slows evaporation [19], the drying step of removal of all free water not bound to glucose is presumably complete within approximately 1 min, or less for higher oven temperatures, thus the majority of the oven duration involves subsequent curing. The curing of this state of two immiscible blended viscous phases, i.e. latex and glucose plasticized by moisture and surfactant from the latex, is analogous to an annealing process in which the latex–glucose interfacial tension drives coarsening of domains of both phases. Glucose is extruded from latex interstices to push the particles into closer and flatter contact, separated by their carboxylic acid coronas to which some glucose remains hydrogen bonded. The latex particles must then overcome this polar barrier for true coalescence to occur via interdiffusion of their styrene–butadiene chain-ends. As glucose content is highest nearer the upper surface, irreversible latex coalescence will tend to be less complete there and channels of expelled glucose will be larger and more prevalent, similar to observations of expulsion of latex-incorporated solution polymer during annealing [20]. While this interfacial tension-driven creeping flow would be expected to maintain connectivity of both "bulk" phases, the occasional occurrence of isolated globules of glucose or latex may be expected. If curing duration suffices, a completely separated layer of glucose external to the upper latex surface will be manifested to globally minimize interfacial area [14]. On removal of the sample from the oven, no further redistribution or coalescence can take place. Immersion in the water bath will leach out the (non-oxidized) glucose and redisperse any non-coalesced latex particles, also removing any partially or fully coalesced latex aggregate globules isolated from their main framework by surrounding glucose. Any disconnected glucose domains will also be vacated, albeit more slowly, by transport through gaps thus created or permeation through partially coalesced surrounding latex.

These mechanisms qualitatively account for the observed trends in yield, light absorbance and morphology. For low temperature and short duration (relative to the given glucose/latex content) the uniform honeycomb of interstitial glucose prohibits sufficient coalescence for percolation of locally film-formed latex, resulting in low yields. For somewhat higher temperatures and/or longer durations the increased coalescence produces latex films with predominantly interstitial porosity, and apparently relatively uniformly so throughout the thickness, as in the bottom row of Fig. 4 and as obtained in other studies [11–14]. Further increase in temperature instills a strong gradient in glucose content during drying, robbing from the lower surface to produce large connected domains near the upper surface, en route to complete phase separation during curing. Thus at these higher temperatures the porous latex film always exhibits low porosity at its lower surface, and can give high or low porosity and pore size at its upper surface depending on the curing duration (Figs. 3 and 4). In the absence of cross-sectional imaging the gradient profile between these two surfaces is not quantitatively known.

The porous latex structures obtained at higher temperatures are structurally similar in pore dimension and morphology to macroporous resin beads prepared by incorporating a pore forming agent, or porogen solvent, during copolymerization [21]. As free-radical copolymerization of monomers with multifunctional cross-linking agents proceeds, their solubility in the porogen solvent diminishes and phase separation occurs, to yield a porous polymer network on removal of the porogen. Such preparations are also prone to creating a difference between internal and external porosity, in particular a non-porous skin layer [21], i.e. the reverse of our films. Analogies also exist with macroporous polymer monoliths obtained from melt blends of immiscible polymers via annealing and post-removal of one phase with a selective solvent. Imposition of a spatially controlled temperature differential during annealing of such systems, grading from coarser to finer domains with decreasing temperature across the sample, can produce gradient porous structures [22]. The approach of the present study facilitates attainment of such structures with finer pores and graded over much thinner films, without the need to physically impose the gradient driving force by contact.

The method of preparing porous latex films via pore forming agents could conceivably be scaled-up to continuous production by coating the dispersion on a moving belt, tuning the convective and/or radiation drying to yield the desired degree of film formation and gradient across the thickness, removing the sugar via a water bath for recycling, and cleanly separating wet film from carrier belt. The dry film maintains its porous structure provided the polymer remains in its glassy state. On exposure to ambient temperatures exceeding its film formation temperature the polymer coalesces to eradicate the intervening pores, at a rate and to an extent dependent on this temperature difference. Similar responses are induced by exposure to liquids or vapors capable of swelling the polymer network and dissolving the non-crosslinked fraction. This progressive loss of opacity may offer possibilities for applications as temperature or chemical sensors. Furthermore, these relatively inexpensive porous films, either in intact form or agitated to an aqueous suspension of porous film particles, may provide a means to enhance the joint strength of interfaces between solution-cast polymer layers. Incorporation of the pre-made porous particles near the surface of one polymer phase, and partially penetrated by it, would present a plethora of microscopically intertwined sites for penetrating and interlocking the second overlain polymer phase to provide adhesion even in the case of phases with very poorly matched surface chemistries.

5. Conclusions

In this study a commercial styrene–butadiene latex dispersion and glucose were combined to demonstrate an augmented scope for pore forming agents to prepare macroporous films of glassy polymer. The aqueous mixture of the two components remains stable and with relatively low viscosity at the high latex loading of 37.5 wt% and glucose/latex proportions (dry/dry) of 15–30%, corresponding to total solids concentrations of 43–49 wt%. The mixtures are well-suited to producing uniform wet coats on substrates of intermediate to high surface energy, partly owing to the surface tension-lowering effect of the surfactants present in the latex dispersion. Drying and curing the wet coats at temperatures exceeding the minimum film formation temperature produces transparent uniform hybrid films. Too low temperature or short duration leads to retention of the sugar in thin layers sheathing the latex particles to inhibit their coalescence, while too high temperatures or long durations lead to complete demixing into separate latex and sugar layers. Drying and curing conditions intermediate to these extremes allow the locking-in of thermodynamically unstable states in which the latex forms a connected, locally film-formed framework surrounded by connected labyrinths of sugar. For such conditions exposure of the film to water leads to rapid elution of the sugar with only minimal redispersion and loss of latex, yielding a porous latex film resisting collapse on ambient drying. While similar procedures in the literature tend to yield partially coalesced, contact-fused sphere packings with small interstitial pores, our approach directed at higher temperatures and using smaller-sized latex yields both more complete coalescence and larger pore channels. The sub-micron pore networks are irregular and disordered, and typically display a gradient in the film thickness direction.

These inexpensive, porous films are suited to applications requiring a transition from opaque to transparent states due to loss of porosity in response to temperature or solvent vapor.

Acknowledgements

Jouko Vyorykka and Pekka Salminen at Dow Chemical are thanked for donation of the latex sample, as is the CRC for Functional Communication Surfaces for a study grant.

References

[1] Y. Chevalier, C. Pichot, C. Graillat, M. Joanicot, K. Wong, J. Maquet, P. Lindner, B. Cabane, Film formation with latex-particles, Colloid Polym. Sci. 270 (1992) 806–821.
[2] M.A. Winnik, Latex film formation, Curr. Opinion Colloid Interface Sci. 2 (1997) 192–199.
[3] J.L. Keddie, Film formation of latex, Mater. Sci. Eng. 21 (1997) 101–170.
[4] A.F. Routh, W.B. Russel, Horizontal drying fronts during solvent evaporation from latex films, AIChE J. 44 (9) (1998) 2088–2098.
[5] A.F. Routh, W.B. Russel, A process model for latex film formation: limiting regimes for individual driving forces, Langmuir 15 (1999) 7762–7773.
[6] P.A. Steward, J. Hearn, M.C. Wilkinson, An overview of polymer latex film formation and properties, Adv. Colloid Interface Sci. 86 (2000) 195–267.
[7] I. Ludwig, W. Schabel, M. Kind, J.-C. Castaing, P. Ferlin, Drying and film formation of industrial waterborne lattices, AIChE J. 53 (3) (2007) 549–560.
[8] E. Lehtinen (Ed.), Pigment Coating and Surface Sizing of Paper, Papermaking Science and Technology, vol. 11, Fapet Oy, Helsinki, 2000.
[9] A. Stein, R.C. Schroden, Colloidal crystal templating of three-dimensionally ordered macroporous solids: materials for photonics and beyond, Curr. Opin. Solid State Mater. 5 (2001) 553–564.
[10] Y. Ma, H.T. Davis, L.E. Scriven, Microstructure development in drying latex coatings, Prog. Org. Coat. 52 (2005) 46–62.
[11] Z. Huang, V.S. Thiagarajan, O.K. Lyngberg, L.E. Scriven, M.C. Flickinger, Microstructure evolution in polymer latex coatings for whole-cell biocatalyst application, J. Colloid Interface Sci. 215 (1999) 226–243.
[12] O.K. Lyngberg, C. Solheid, S. Charaniya, Y. Ma, V. Thiagarajan, L.E. Scriven, M.C. Flickinger, Permeability and reactivity of Thermotoga maritima in latex bimodal blend coatings at 80 °C: a model high temperature biocatalytic coating, Extremophiles 9 (2005) 197–207.
[13] P.A. Steward, J. Hearn, M.C. Wilkinson, Studies on permeation through polymer latex films. 2. Permeation modification by sucrose addition, Polym. Int. 38 (1) (1995) 13–22.
[14] I.C. Hodges, J. Hearn, Reactive latex films, Langmuir 17 (2001) 3419–3422.
[15] L.E. Appel, G.M. Zentner, Use of modified ethylcellulose lattices for microporous coating of osmotic tablets, Pharm. Res. 8 (5) (1991) 600–604.
[16] A.D. Dinsmore, M.F. Hsu, M.G. Nikolaides, M. Marquez, A.R. Bausch, D.A. Weitz, Colloidosomes: selectively permeable capsules composed of colloidal particles, Science 298 (2002) 1006–1009.
[17] M. Braga, M. da Silva, A.H. Cardoso, F. Galembeck, Latex surface and bulk coagulation induced by solvent vapors, J. Colloid Interface Sci. 228 (2000) 171–177.
[18] Y. Chen, W.T. Ford, N.F. Materer, D. Teeters, Conversion of colloidal crystals to polymer nets: turning latex particles inside out, Chem. Mater. 13 (2001) 2697–2704.
[19] S.A. Cooke, S.O. Jonsdottir, P. Westh, A thermodynamic study of glucose and related oligomers in aqueous solution: vapor pressures and enthalpies of mixing, J. Chem. Eng. Data 47 (2002) 1185–1192.
[20] Y.J. Park, D.Y. Lee, M.C. Khew, C.C. Ho, J.H. Kim, Effects of alkali-soluble resin on latex film morphology of poly(n-butyl methacrylate) studied by atomic force microscopy, Langmuir 14 (1998) 5419–5424.
[21] S. Dubinsky, J.I. Park, I. Gourevich, C. Chan, M. Deetz, E. Kumacheva, Towards controlling the surface morphology of macroporous copolymer particles, Macromolecules 42 (2009) 1990–1994.
[22] D. Yao, W. Zhang, J.G. Zhou, Controllable growth of gradient porous structures, Biomacromolecules 10 (2009) 1282–1286.